

Fabrication of biomorphic SiC composites using wood preforms with different structures

Dong J. Lee^a, Jong J. Jang^a, Hee S. Park^a, Yun C. Kim^b,
Kwang H. Lim^c, Sang B. Park^d, Soon H. Hong^{a,*}

^aDepartment of Materials Science and Engineering, KAIST, 291 Daehak-ro, Yuseong-Gu, Daejeon 307-701, Republic of Korea

^bAgency for Defense Development, Yuseong-gu, Daejeon 305-152, Republic of Korea

^cDaeyang Ind., Co., Icheon-city, Gyeonggi-do 467-813, Republic of Korea

^dKorea Forest Research Institute, Dongdaemun-gu, Seoul 130-712, Republic of Korea

Received 20 November 2011; received in revised form 2 December 2011; accepted 2 December 2011

Available online 27 December 2011

Abstract

Biomorphic SiC composites were fabricated from wood, including high-density compressed cedar, high-density fiberboard (HDF) and low-density paulownia followed by the fabrication of a preform and liquid silicon infiltration (LSI) process. The degree of molten silicon infiltration was strongly dependent on the cell wall thickness and pore size of the carbon preform. The mechanical properties of the biomorphic SiC composites were characterized by compressive tests at room temperature, 1000 °C and 1200 °C, and the relationship between the mechanical properties and the microstructural characteristics was analyzed. The compressive strength of the biomorphic composites was found to be strongly dependent on their bulk density and decreased as the test temperature increased to 1200 °C. Strength reduction in the biomorphic SiC composites occurred due to the deformation of the remaining Si at elevated temperatures under ambient atmospheric conditions.

© 2011 Elsevier Ltd and Techna Group S.r.l. All rights reserved.

Keywords: B. Composites; D. SiC; E. Refractories; Mechanical characterization

1. Introduction

SiC composites have good specific strength, thermal shock resistance, ablation resistance and oxidation resistance at high temperatures. Accordingly, SiC composites are regarded as excellent thermal protection materials. A number of manufacturing processes have been used to fabricate these novel materials, including hot pressing, reaction bonding, reaction forming, polymer pyrolysis and chemical vapor deposition processes. However, due to the environmental and economic issues associated with traditional manufacturing processes, there is now a great interest in efforts to utilize biomimetic approaches to fabricate SiC composites [1]. Biomorphic SiC composites have several benefits over traditional SiC composites. One benefit is that they require less energy to manufacture due to the low fabrication temperatures. Another benefit is the wide variety of microstructures that can be

obtained, as determined by the morphology of the template biomaterials [2].

Wood exhibits excellent strength with low density, high stiffness, elasticity and damage tolerance on micro and macro scales. Regarding the structural aspects of wood, it is typically composed of cellulose, hemicellulose and lignin, all of which can decompose and produce a three-dimensional structure of amorphous carbon during a pyrolysis process. Because wood, when used in carbon preforms can maintain good mechanical properties after a pyrolysis process, it is possible to fabricate low-cost biomorphic SiC composites from wood [3,4].

Research into biomorphic SiC ceramics has concentrated on the microstructural conversion of biomaterials by different fabrication processes. For example, Greil et al. [3,4], Varela-Feria et al. [5], Hou et al. [6], and Weisensel et al. [7] fabricated biomorphic SiC ceramics derived from various natural woods using liquid silicon infiltration (LSI) processes. Volgi et al. [8] and Rambo et al. [9] attempted to use a Si vapor infiltration process and a sol–gel process to fabricate porous SiC ceramics. Streitwieser et al. [10] fabricated porous SiC ceramics using a chemical vapor infiltration (CVI) process.

* Corresponding author. Tel.: +82 42 350 3327; fax: +82 42 350 3310.

E-mail address: shhong@kaist.ac.kr (S.H. Hong).

The low density of carbon preforms is responsible for the presence of a large amount of residual Si in the final composites during the LSI process. The mechanical properties of biomorphic SiC composites decrease at high temperatures due to these residual Si phases, which have a low melting temperature of about 1410 °C. As yet, there have been few attempts to decrease the amount of residual Si in biomorphic SiC composites [7].

In this study, in an effort to reduce the amount of Si remaining in the final product, molten Si was infiltrated into high-density carbon preforms, in this case high-density fiberboard (HDF) and compressed cedar, which were fabricated by wood compression and pyrolysis processes [11]. HDF is an artificial wood product created by powdering wood, mixing the powder with binders, and finally forming the product under high pressure and at high temperatures [12]. Unlike natural wood, it is possible to use HDF to fabricate homogeneous and consistent high-density preforms. A biomorphic composite derived from paulownia, a low-density wood, was also manufactured for comparison with the composites from the high-density woods. During each process, the microstructures of the starting woods, the carbon preforms, and the composites were analyzed. The mechanical properties and oxidation behaviors of the composites were also characterized.

2. Experimental procedures

2.1. Selection of wood and fabrication process

Rectangular specimens (100 mm × 100 mm × 10 mm) were cut from paulownia, HDF and compressed cedar. These wood samples were dried at 100 °C for 24 h in a vacuum oven. The dried wood specimens were converted to carbon preforms by a pyrolysis process at 1000 °C in an atmosphere of flowing nitrogen. The weight loss and shrinkage rate in each direction were evaluated after the pyrolysis process.

Molten Si was infiltrated into the carbon preforms in a graphite furnace under a vacuum at 1560 °C for 40 min. To produce biomorphic SiC composites of full density, excess Si over the stoichiometric amount (234 wt.%) is necessary. Therefore, 4–10 times the weight ratio of the starting silicon to the carbon preform (W_{Si}/W_C) was arranged. After the silicon infiltration process, the specimens were machined in order to characterize their mechanical properties. Details of the fabrication procedures are described in our previous report [13].

2.2. Characterization

The characterization of the wood decomposition behavior was performed with a thermogravimetric analyzer (TG, Netzsch TG 209 F3), and the characterization of the reaction between the carbon preform and the silicon was performed using a differential scanning calorimetry analyzer (DSC, Netzsch DSC 204 F1). The microstructures of the carbon preform and the composites were observed by scanning electron microscopy (SEM, Philips XL30SFEG) and optical microscopy (Leica, DC-200). The phases of the carbon

preforms and the composites were analyzed by X-ray diffraction analysis (XRD, Rigaku D/Max-IIIC (3 kW)). The bulk density and porosity of the preforms and composites were measured using the Archimedes method (ASTM 373-88) [14] and with a porosimeter (Micromeritics, Autopore-IV 9520). To analyze the composition of the composites, the remaining Si was removed using a solution of hydrofluoric and nitric acids and the remaining carbon was removed by oxidation at 1200 °C in air [15]. Then, compressive tests were performed according to ASTM C 773-88 [16] using a universal testing machine (INSTRON 5583).

3. Results and discussion

3.1. Fabrication of carbon preforms

The wood pyrolysis process involves a series of overlapping decompositions of biopolymers. To investigate the decomposition behavior, small pieces of wood were heated in a thermogravimetric analyzer to 1000 °C at a furnace rate of 10 °C/min under a flowing nitrogen atmosphere. Fig. 1(a) shows the thermogravimetric analysis (TGA) results of three different types of wood. There are similarities in the decomposition reactions. The initial weight loss most likely occurred due to the removal of moisture. Hemicellulose was smoothly decomposed

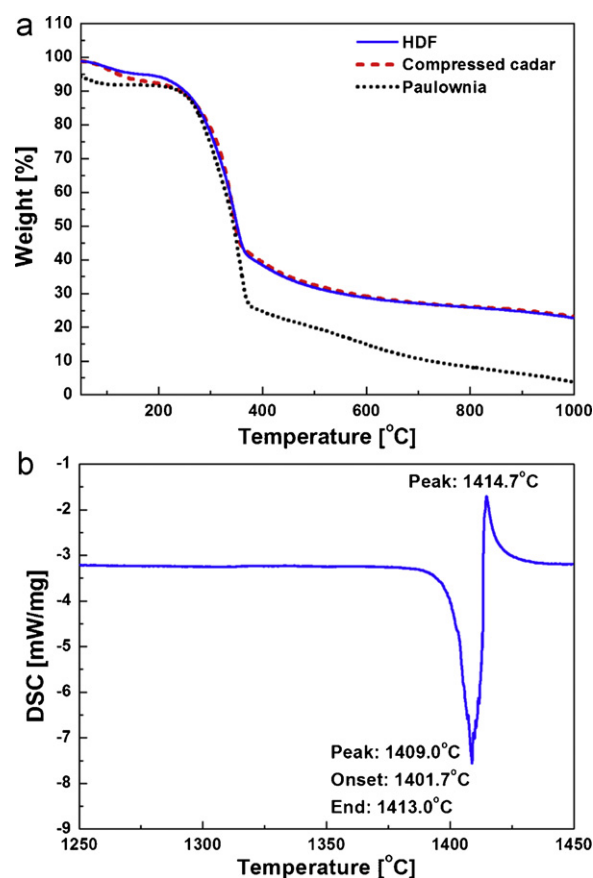


Fig. 1. (a) Thermogravimetric analysis (TGA) curves of three different kinds of wood. (b) Differential scanning calorimetry (DSC) curves for the formation of silicon carbide from carbon preform and silicon.

Table 1

Microstructural characteristics of the wood, the carbon preforms and the biomorphic composites.

| | Woods | Perform | | Composites | | | | | |
|------------------|------------------------------|------------------------------|--------------|------------|-----------|----------|-----------------------------------|--|----------------------|
| | Density (g/cm ³) | Density (g/cm ³) | Porosity (%) | SiC (wt.%) | Si (wt.%) | C (wt.%) | Bulk density (g/cm ³) | Theoretical density (g/cm ³) | Relative density (%) |
| Paulownia | 0.29 | 0.17 | 80.7 | 63.4 | 34.7 | 2.0 | 2.36 | 2.88 | 81.9 |
| Compressed cedar | 1.10 | 0.82 | 34.1 | 80.2 | 12.5 | 7.3 | 2.77 | 3.01 | 92.0 |
| HDF | 1.15 | 0.98 | 28.6 | 79.4 | 16.6 | 4.0 | 2.95 | 2.99 | 98.6 |

around 190–250 °C and volatile products (CO₂, CO and organic vapors) were released. Major weight loss occurred in temperature range of 250–360 °C due to the decomposition of cellulose and lignin [1,2]. Almost all of the cellulose was decomposed while the lignin was gradually decomposed until finally 3–23 wt.% of solid carbon remained at 1000 °C.

Wood specimens were pyrolyzed at 1000 °C under a flowing nitrogen atmosphere. Although anisotropic shrinkage occurred during the pyrolysis process, the carbon preforms retained their original shape. The characteristics of the wood samples and the carbon preforms are summarized in Table 1. The microstructural characteristics of the carbon preforms were similar to those of the wood samples, as shown in Fig. 2. The carbon preform derived from paulownia had thin cell walls and a heterogeneous pore size and distribution. The latewood area of the compressed cedar preform had thick cell walls and small pores that were homogeneously distributed. The earlywood area of the cedar preform had large pores and thin cell walls; however, the large pores were compressed during the compression process. Therefore, the compressed cedar preforms were denser than those of natural cedar.

3.2. Fabrication of SiC composites

To study the reactions between the carbon preforms and silicon, charcoal and Si powder were heated in a differential scanning calorimeter to 1450 °C at a heating rate of 10 °C/min under a flowing argon atmosphere. The melting of the Si started at 1401.7 °C and finished at 1413.0 °C with an endothermic reaction. The formation of SiC occurred at 1414.7 °C with an exothermic reaction, as shown in Fig. 1(b).

During the LSI process, spontaneous wetting and infiltration occurred when molten Si came into contact with the carbon perform [3]. The heterogeneous chemical reaction process was a combination of mass transfer from the reactant (Si) to the solid (C) surface, diffusion through the reaction products (SiC) and the chemical reaction of Si and C. Infiltration of the molten Si into the tracheidal pores was completed in a few seconds due to the almost complete wetting of molten Si on the carbon surface. Therefore, it can be seen that this reaction is dominated by diffusion. Assuming that it is a diffusion-controlled reaction, the thickness of the reaction layer can be expressed by the equation below.

$$d_{\text{SiC}} = \sqrt{D_0 \exp\left(\frac{-E}{RT}\right) t} \quad (1)$$

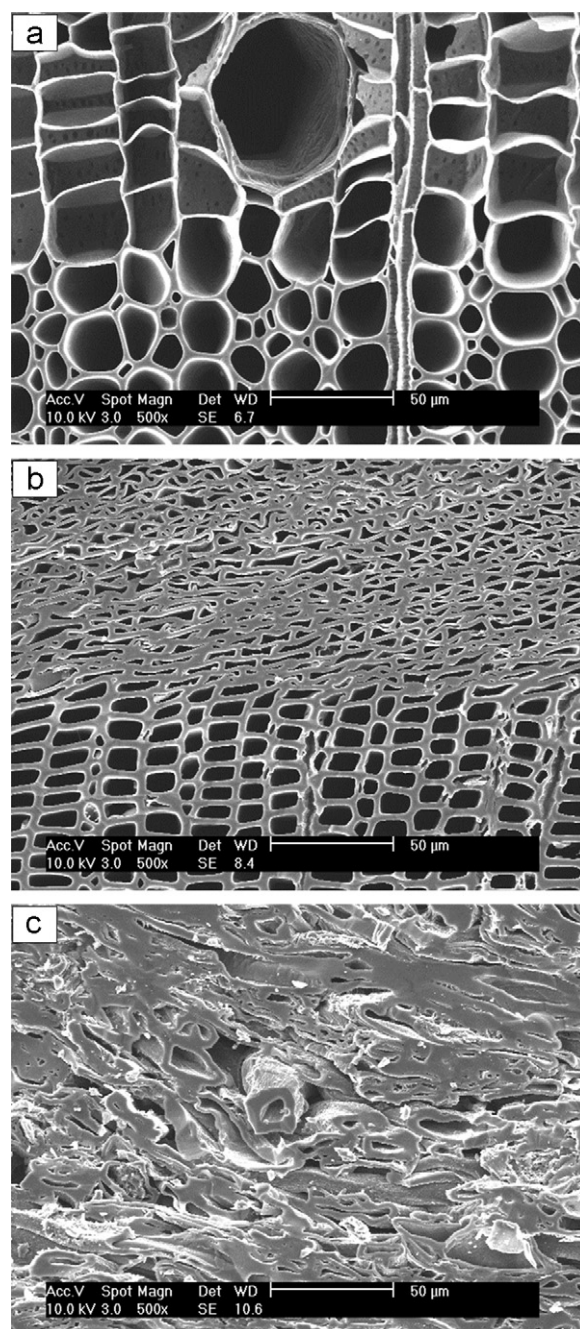


Fig. 2. SEM micrographs showing cross-sections of carbon preforms made from (a) paulownia, (b) compressed cedar, and (c) HDF.

Using Eq. (1), the reaction time for the complete formation of SiC can be derived as follows:

$$t_R = \frac{d_{\text{SiC}}^2}{D_0 \exp(-E/RT)} \quad (2)$$

The reaction time can be estimated as 48 min with the activation energy $E = 132$ kJ/mol, the diffusion rate $D_0 = 2.0 \times 10^{-6}$ cm²/s, the processing temperature $T = 1833$ K and the maximum thickness of the carbon layer which is converted into SiC $d_{\text{SiC}} = 10$ μm [17].

After silicon infiltration, the carbon preforms were converted into SiC and mostly retained their original structures. Pores were filled with residual Si, but some large pores were not filled with Si due to the low surface tension of large pores. Residual carbon was found in tiny pores with thick carbon cell wall regions. During the SiC formation reaction, the volume increased and the pores were closed before all of the carbon had been converted into SiC [18]. Fig. 3 shows the cross-sections of the biomorphic SiC composites from three different wood samples, where the grey area is SiC, the white area is residual silicon, the dark grey area is residual carbon, and the black area indicates pores. Some large pores in the region of the paulownia with thin cell walls lost their three-dimensional structure during the rapid exothermic reaction of Si and carbon. Compressed cedar-based composites were clearly distinguished into rich Si (the latewood area) and rich SiC zones (the compressed area from earlywood). Although residual carbon was generally observed in the latewood area due to the thick cell walls and small pores corresponding to the low growth rate of the wood, residual carbon was also observed in the earlywood area with thin cell walls but with tiny pores resulting from the compression process undergone by the wood. Although the density of the carbon preform made from compressed cedar is lower than that made from HDF, the residual carbon content of the final composite is higher than that of HDF, as can be seen in the results summarized in Table. 1. This indicates that the compressed cedar preform has more numerous small pores, which makes it difficult for molten silicon to infiltrate.

3.3. Mechanical properties

The compressive strength of composites derived from high-density woods was almost two times higher than the strength of composites derived from low-density wood. Fig. 4(a) shows the compressive strength as a function of the bulk density, showing that it is a linear function of the bulk density. The denser SiC composites show higher compressive strength. This result is in good agreement with previous results regarding the compressive strength of biomorphic SiC ceramics [18].

The compressive strength of the biomorphic SiC composites is plotted in Fig. 4(b) as a function of the temperature. The HDF-based composites exhibited substantially higher strength at all temperatures due to the high bulk density. At the temperature range of RT–1000 °C, the compressive strength of the biomorphic SiC composites was maintained, whereas the compressive strength of the HDF-based composites and the paulownia-based composites drastically decreased when the

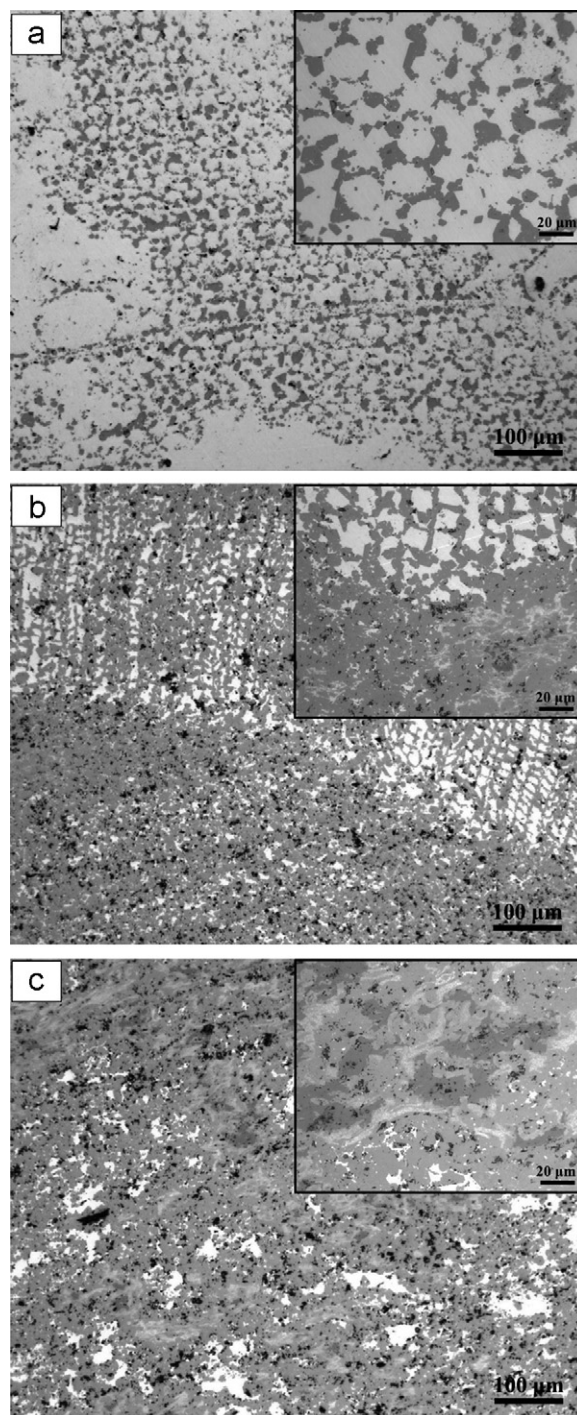


Fig. 3. Optical micrographs showing cross-sections of biomorphic SiC composites derived from (a) paulownia, (b) compressed cedar, and (c) HDF.

temperature exceeded 1000 °C. The compressive strength loss in the SiC composites was associated with the softening of the remaining Si at the elevated temperature. The fracture surfaces of the HDF-based composites and paulownia-based composites SiC composites as shown in Fig. 5(a) and (c) exhibited a softening of the remaining Si at 1200 °C due to their high Si contents.

There is rapid strength loss over 1000 °C, which temperature is approaching the melting point of Si, due to the softening of

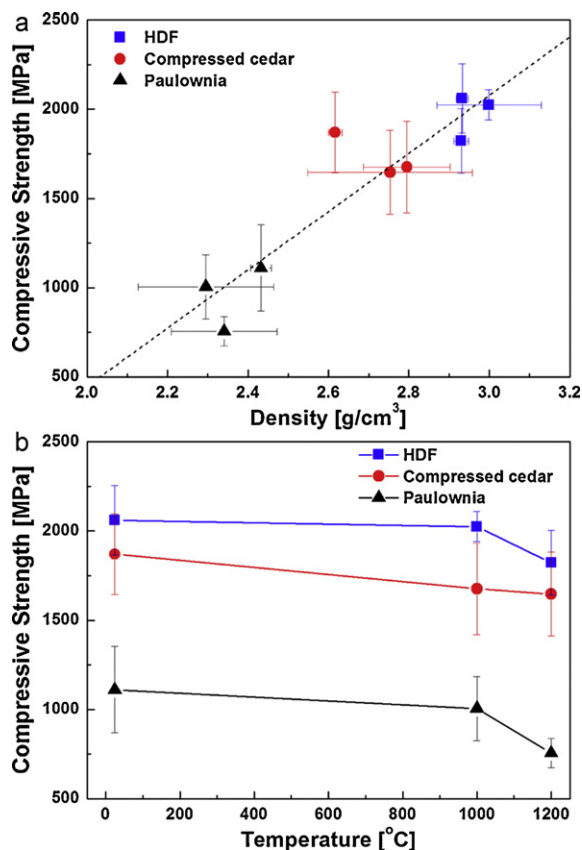


Fig. 4. (a) Influence of the bulk density on the compressive strength at room temperature, 1000 °C and 1200 °C under ambient atmospheric conditions. (b) Compressive strength as a function of the temperature for biomorphic SiC composites made from three different types of wood.

the remaining Si. The three-dimensional network structure of SiC starts to lose its connectivity and strength because the residual Si between the SiC grains is deformed plastically at temperatures up to 1200 °C. The loss in the compressive strength occurred in proportion to the amount of remaining Si. Therefore, the greatest strength loss occurred in the paulownia and HDF based composites, which had the highest amount of residual Si, while the lowest amount of strength loss occurred in the compressed cedar-based composites, which had the lowest amount of residual Si.

3.4. Oxidation behavior

To investigate the oxidation behavior of the biomorphic SiC composites, small pieces of composites were heated in a thermogravimetric analyzer to 1200 °C at a furnace rate of 10 °C/min with flowing air. There are several phenomena that control the oxidation kinetics of SiC composites [20]. These are listed below.

- (1) Diffusion of gaseous species through microcracks in the SiC layer.
- (2) Diffusion of the gaseous species through the pores created by the oxidation of residual carbon.
- (3) Diffusion of oxygen at the active sites of the carbon surface.

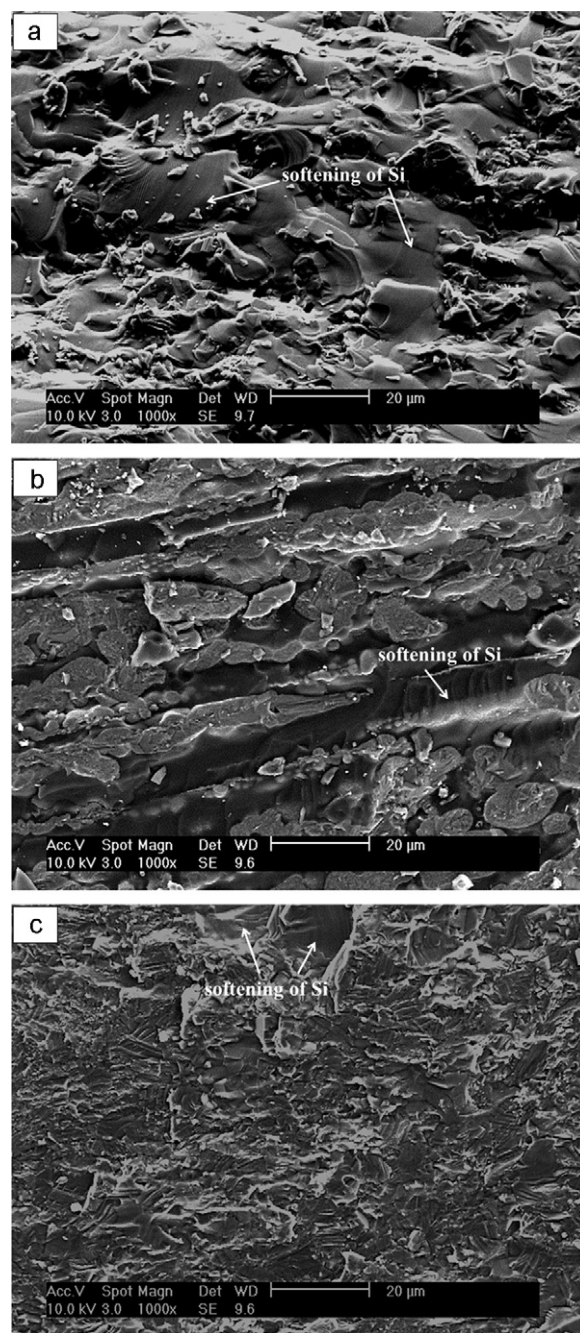


Fig. 5. Fracture surface of biomorphic SiC composites derived from (a) paulownia, (b) compressed cedar and (c) HDF at 1200 °C.

- (4) Reactions between oxygen and carbon according to the following equations:



- (5) Formation of a silica layer during the oxidation of the SiC structure according to the following equations:



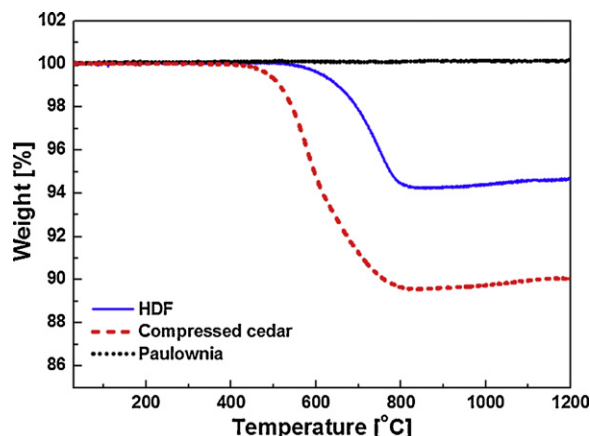


Fig. 6. Thermogravimetric analysis (TGA) curves of three different types of biomorphic SiC composites under ambient atmospheric conditions.

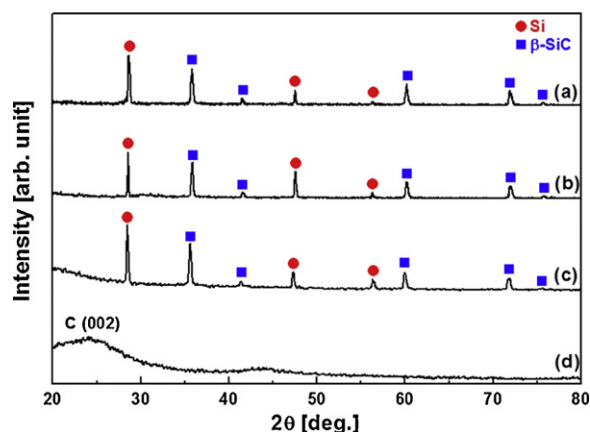


Fig. 7. XRD spectra of (a) oxidized composites at 1200 °C in air, (b) oxidized composites at 1000 °C in air, (c) HDF-based SiC composite, and (d) a carbon preform of HDF.

Previous studies [19] have shown that carbon monoxide is the major oxidation product beyond 700 °C. Therefore, considering the oxidation temperature range of this study (400–800 °C), only Eq. (4) occurred. For the oxidation of SiC, Eq. (6) is more likely to occur than Eq. (5).

The thermogravimetric analysis (TGA) results of the three different composites are shown in Fig. 6. Oxidation of the residual carbon starts around 400 °C and is completed around 800 °C. According to the amount of residual carbon, 0–10.4 wt.% of weight loss occurred, and there was a particularly low level of weight loss in the composites made from paulownia. At temperatures up to 1200 °C, there was 0.1–0.3 wt.% of weight gain due to the oxidation of SiC. Although the composites gained weight due to the oxidation of SiC, the XRD results did not show silica peaks due to the small amount of silica, as shown in Fig. 7. The oxidation of carbon, however, was clearly observed. Fig. 7(d) shows the XRD results of the carbon preform of HDF with broad carbon peaks after silicon infiltration peaks due to the β-SiC phases; silicon phases are observed together with the broad peaks due to the residual carbon. However, during the oxidation of the composites at

temperatures up to 1200 °C, the residual carbon almost completely disappeared, as shown in Fig. 7(a) and (b).

4. Conclusions

Biomorphic SiC composites were fabricated by liquid silicon infiltration of pyrolyzed high-density and low-density types of wood. The microstructure of the carbon preforms and the biomorphic SiC composites retained the natural shape of the wood on which they were patterned. The compressive strength of composites based on high-density wood was almost two times higher than that of composites based on low-density wood. The compressive strength strongly depended on the bulk density. Compressive strength loss occurred due to the softening of residual Si at temperatures up to 1200 °C. The critical factor in ensuring good mechanical properties at high temperatures in biomorphic SiC composites is the maintenance of the stiff SiC structures despite the deformation of residual Si.

Acknowledgements

This research was supported by the Defense Acquisition Program and the Agency for Defense Development under contract UD070033AD and by NSL(National Space Lab) program through the Korea Science and Engineering Foundation funded by the Ministry of Education, Science and Technology (20110018657) and by Priority Research Centers Program through the National Research Foundation of Korea(NRF) funded by the Ministry of Education, Science and Technology (2009-0094039).

References

- [1] M. Singh, J.A. Salem, Mechanical properties and microstructure of biomorphic silicon carbide ceramics fabricated from wood precursors, *J. Eur. Ceram. Soc.* 22 (2002) 2709–2717.
- [2] M. Singh, B.-M. Yee, Reactive processing of environmentally conscious, biomorphic ceramics from natural wood precursors, *J. Eur. Ceram. Soc.* 24 (2004) 209–217.
- [3] P. Greil, T. Lifka, A. Kaindl, Biomorphic cellular silicon carbide ceramics from wood: I. Processing and microstructure, *J. Eur. Ceram. Soc.* 18 (1998) 1961–1973.
- [4] P. Greil, T. Lifka, A. Kaindl, Biomorphic cellular silicon carbide ceramics from wood: II. Mechanical properties, *J. Eur. Ceram. Soc.* 18 (1998) 1975–1983.
- [5] F.M. Varela-Feria, J. Martínez-Fernández, A.R. de Arellano-López, M. Singh, Low-density biomorphic silicon carbide: microstructure and mechanical properties, *J. Eur. Ceram. Soc.* 22 (2002) 2719–2725.
- [6] G. Hou, Z. Jin, J. Qian, Effect of holding time on the basic properties of biomorphic SiC ceramic derived from beech wood, *Mater. Sci. Eng. A* 452 (2007) 278–283.
- [7] L. Weisensel, H. Sieber, Reactive melt infiltration processing of biomorphic Si–Mo–C ceramics from wood, *J. Am. Ceram. Soc.* 88 (2005) 1792–1798.
- [8] E. Volgi, H. Sieber, P. Greil, SiC-ceramic prepared by Si-vapor phase infiltration of wood, *J. Eur. Ceram. Soc.* 22 (2002) 2663–2668.
- [9] C.R. Rambo, J. Cao, O. Rusina, H. Sieber, Manufacturing of biomorphic (Si, Ti, Zr)-carbide ceramics by sol–gel processing, *Carbon* 43 (2005) 1174–1183.
- [10] D.A. Streitwieser, N. Popovska, H. Gerhard, G. Emig, Application of the chemical vapor infiltration and reaction (CVI-R) technique for the preparation of highly porous biomorphic SiC ceramics derived from paper, *J. Eur. Ceram. Soc.* 25 (2005) 817–828.

- [11] I. Abe, T. Fukuhara, S. Iwasaki, K. Yasuda, K. Nakagawa, Y. Iwata, H. Kominami, Y. Kera, Development of a high-density carbonaceous adsorbent from compressed wood, *Carbon* 39 (2001) 1485–1490.
- [12] M. Rowell Roger, *Handbook of Wood Chemistry and Wood Composites*, Taylor & Francis, 2005.
- [13] H.S. Park, J.J. Jang, K.H. Lee, K.H. Lim, S.B. Park, Y.C. Kim, S.H. Hong, Effects of microstructure on flexural strength of biomorphic C/SiC composites, *Int. J. Fracture* 151 (2008) 233–245.
- [14] ASTM C 373-88 Standard test method for water absorption, bulk density, apparent porosity, and apparent specific gravity of fired whiteware products (reapproved 2006).
- [15] V.S. Kaul, K.T. Faber, Nanoindentation analysis of the elastic properties of porous SiC derived from wood, *Scripta Mater.* 58 (2008) 886–889.
- [16] ASTM C 773-88 Standard test method for compressive (crushing) strength of fired whiteware (reapproved 2006).
- [17] E. Fitzer, R. Gadow, Fiber-reinforced silicon carbide, *J. Am. Ceram. Soc.* 65 (1986) 326–335.
- [18] M. Presas, J.Y. Pastor, J.L. Lorca, A.R. de Arellano-López, J. Martínez-Fernández, R.E. Sepúlveda, Mechanical behavior of biomorphic Si/SiC porous composites, *Scripta Mater.* 53 (2005) 1175–1180.
- [19] F. Lamouroux, G. Camus, J. Thébault, Kinetics and mechanisms of oxidation of 2D woven C/SiC composites: I. Experimental approach, *J. Am. Ceram. Soc.* 77 (8) (1994) 2049–2057.
- [20] F. Lamouroux, R. Naslain, J.-M. Jouin, Kinetics and mechanisms of oxidation of 2D woven C/SiC composites: II. Theoretical approach, *J. Am. Ceram. Soc.* 77 (8) (1994) 2058–2068.